

Supporting Information for

Double Gyroid-Structured Electrolyte based on an Azobenzene-Containing Monomer and Its Polymer

Dong Liu,^{a&} Shangming He,^{b&} Longfei Luo,^a Weilu Yang,^a Yun Liu,^a Shichu Yang,^a Zhihao Shen,^{a} Shuangjun Chen^b and Xinghe Fan^{a*}*

^aBeijing National Laboratory for Molecular Sciences, Key Laboratory of Polymer Chemistry and Physics of Ministry of Education, Center for Soft Matter Science and Engineering, College of Chemistry and Molecular Engineering, Peking University, Beijing, 100871, China

^bCollege of Materials Science & Engineering, Nanjing Tech University, Nanjing, 210009, China.

[&]These authors contributed equally to this work and should be considered co-first authors

Table of Contents

Materials	S3
Synthesis	S3
Methods	S6
Results	S7
Figure S1. ¹ H NMR, ¹³ C NMR, and MS spectra of NbAzo	S7
Figure S2. ¹ H NMR spectrum of PAzo	S8
Figure S3. SEC curves of PAzo	S8
Figure S4. TGA thermograms of PAzo	S9
Figure S5. DSC curves of PAzo-31.5k and PAzo-31.5k/NbAzo/LiTFSI with r_{Li} of 0.66	S9
Figure S6. MAXS profiles of PAzo-31.5k/NbAzo/LiTFSI with different r_{Li}	S10
Figure S7. Schematic illustration of LAM and LAM1 + LAM2	S11

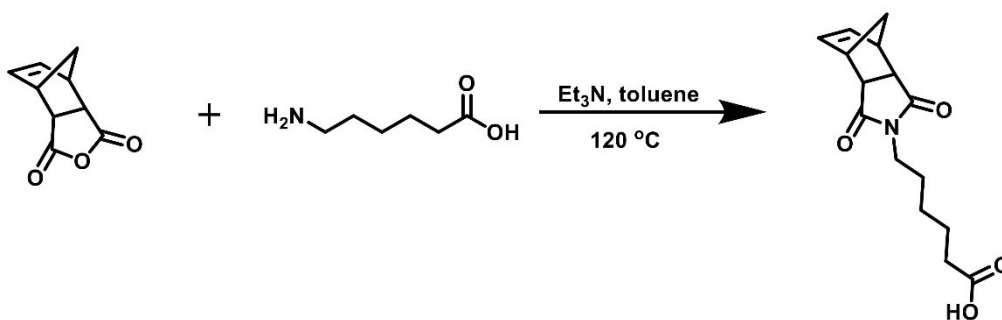
Figure S8. MAXS profiles of PAzo/NbAzo/LiTFSI ($r_{\text{Azo}} = 0.067\text{--}0.53$)	S12
Figure S9. MAXS profiles of PAzo/NbAzo/LiTFSI ($r_{\text{Azo}} = 0.60\text{--}1.30$)	S12
Figure S10. MAXS profiles of PAzo/NbAzo/LiTFSI ($r_{\text{Azo}} = 1.40\text{--}1.80$)	S13
Figure S11. PLM results of PAzo-31.5k at different temperatures	S14
Figure S12. MAXS profiles of PAzo-72.1k and PAzo-63.2k/NbAzo/LiTFSI	S15
Figure S13. Apparent phase diagrams of PAzo/NbAzo/LiTFSI	S15
Figure S14. MAXS and WAXS profiles of NbAzo	S16
Figure S15. MAXS and WAXS profiles of PAzo/LiTFSI, NbAzo/LiTFSI, and PAzo/NbAzo	S16
Figure S16. Temperature-dependent ionic conductivities of PAzo-18.2k/NbAzo/LiTFSI	S17
Figure S17. Measurement of the transference number of PAzo-31.5k/NbAzo/LiTFSI	S17

Materials

Dichloromethane (CH₂Cl₂, HPLC grade), toluene (HPLC grade), and tetrahydrofuran (THF, HPLC grade) were purified with an M Braun SPS-800 solvent processing system to remove dissolved oxygen and water. Lithium bistrifluoromethanesulfonimide (LiTFSI) was kept at 110 °C in vacuum for at least 24 h before use. Phenol, 4-*n*-butylaniline, 1-ethyl-3-(3-dimethylamino-propyl) carbodiimide hydrochloride (EDC•HCl), and 4-(dimethylamino) pyridine (DMAP) were purchased from Macklin Inc. All other reagents were used as received without any purification.

Synthesis

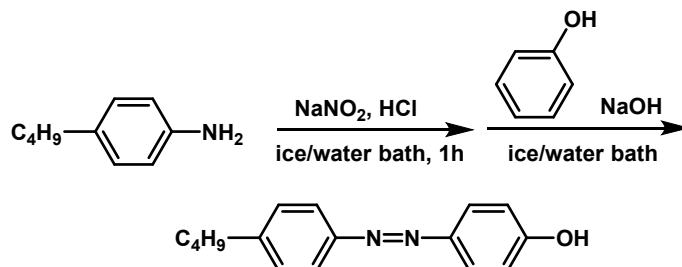
Synthesis of NbCOOH. The synthetic route is shown in Scheme S1. *cis*-5-Norbornene-*exo*-2,3-dicarboxylic anhydride (1.00 eq, 4.00 g, 24.4 mmol), 6-aminocaproic acid (1.00 eq, 3.20 g, 24.4 mmol), trimethylamine (0.100 eq, 0.340 mL, 2.44 mmol), and 60 mL of toluene were added into a 100 mL flask. After being refluxed at 120 °C for 12 h, the solution was condensed, and 50 mL of CH₂Cl₂ was added. The solution was washed with water and brine three times and dried with Na₂SO₄. The white solid was collected after the removal of the solvent.



Scheme S1. Synthesis of NbCOOH.

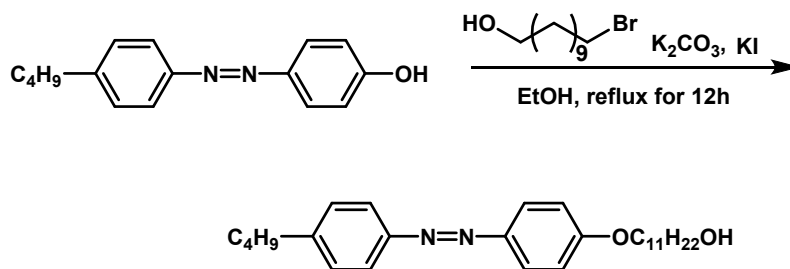
Synthesis of C4AzoOH. The synthetic route is shown in Scheme S2. 4-*n*-Butylaniline (3.14 g, 21.0 mmol), HCl (12 M, 5.30 mL, 63.0 mmol), and 50 mL of deionized water were added into a 250 mL flask with a stir bar, and then the above solution was put in an

ice/water bath. Sodium nitrite (1.76 g, 25.0 mmol) dissolved in 40 mL of deionized water was added dropwise to the above solution. And then the mixed solution reacted for another hour to form the solution A. Phenol (2.17 g, 23.0 mmol), sodium hydroxide (0.840 g, 21.0 mmol), sodium carbonate (2.25 g, 21.0 mmol), and 50 mL of deionized water were charged into a 250 mL flask with a stir bar, and then the mixture was cooled to below 5 °C to obtain the solution B. Solution A was slowly added into the solution B, which was kept in an ice/water bath. After the addition, the ice/water bath was removed, and the mixed solution reacted at ambient temperature for 2 h. After the reaction was completed, the reaction solution was neutralized with dilute hydrochloric acid. The resulting precipitate was filtered, washed with deionized water, and dried to give a crude product. The crude product was recrystallized from petroleum ether to give a dark yellow solid. Yield: 90%. ¹H NMR (400 MHz, CDCl₃, δ, ppm): 7.87 (m, 2H), 7.81 (m, 2H), 7.30 (m, 2H), 6.94 (m, 2H), 2.68 (t, 2H), 1.64 (m, 2H), 1.38 (h, 2H), 0.94 (t, 3H).



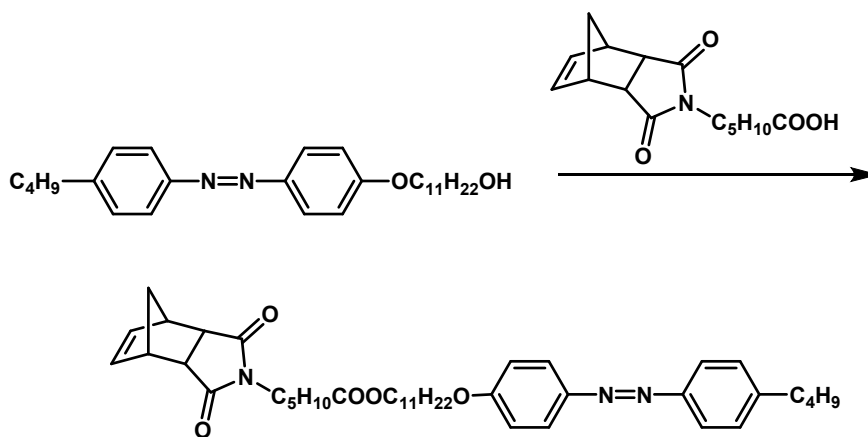
Scheme S2. Synthesis of C4AzoOH.

Synthesis of C4AzoC11OH. The synthetic route is shown in Scheme S3. C4AzoOH (5.08 g, 20.0 mmol), 11-bromo-1-undecyl alcohol (5.02 g, 20.0 mmol), potassium iodide (35.2 mg, 0.200 mmol), potassium carbonate (11.0 g, 80.0 mmol), and 150 mL of anhydrous ethanol were filled into a flask with a stir bar, and then the mixture was refluxed overnight. After filtration, the crude product was recrystallized from anhydrous ethanol to give bright yellow crystals. Yield: 80%. ¹H NMR (400 MHz, CDCl₃, δ, ppm): 7.89 (m, 2H), 7.80 (m, 2H), 7.30 (m, 2H), 6.99 (m, 2H), 4.03 (t, 2H), 3.64 (t, 2H), 2.68 (t, 2H), 1.80 (m, 2H), 1.25–1.69 (m, 21), 0.94 (t, 3H).



Scheme S3. Synthesis of C4AzoC11OH.

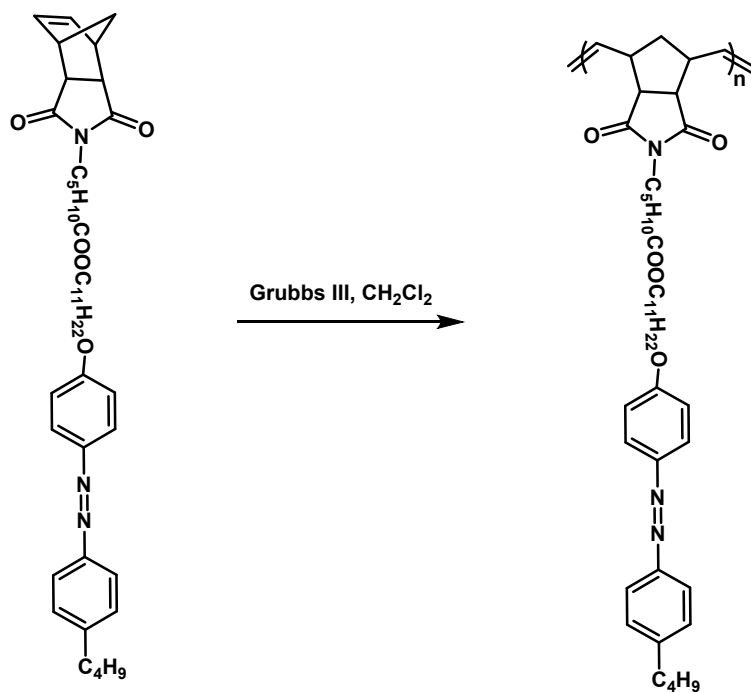
Synthesis of NbAzo. The synthetic route is shown in Scheme S4. NbCOOH (1.20 eq, 1.97 g, 7.12 mmol), polyethylene glycol monomethyl ether ($M_n = 950 \text{ g mol}^{-1}$, 1.00 eq, 3.20 g, 24.4 mmol), and 80 mL of CH_2Cl_2 were added into a 150 mL flask. 1-Ethyl-3-(3-dimethylamino-propyl)carbodiimide hydrochloride (EDC•HCl, 2.40 eq, 2.72 g, 14.2 mmol), and 4-(dimethylamino)pyridine (DMAP, 0.200 eq, 0.145 g, 1.18 mmol) were added into the solution slowly. After being stirred at ambient temperature for 36 h, the solution was condensed and washed with 1 M HCl aqueous solution. Then the resulting solution was washed with brine three times and dried with Na_2SO_4 . the crude product was recrystallized from anhydrous ethanol to give bright yellow crystals. $^1\text{H NMR}$ (400 MHz, CDCl_3 , δ , ppm): 7.90 (m, 2H), 7.81 (m, 2H), 7.30 (m, 2H), 7.00 (m, 2H), 6.28 (m, 2H), 4.04 (t, 4H), 3.46 (t, 2H), 3.26 (m, 2H), 2.68 (t, 4H), 2.29 (t, 2H), 1.82 (m, 4H), 1.25–1.69 (m, 24H), 0.94 (t, 3H).



Scheme S4. Synthesis of NbAzo.

Methods

Polymerization of NbAzo. PAzo was polymerized through ring-opening metathesis polymerization (ROMP) (Scheme S5). A typical synthetic process is described below. Grubbs III catalyst (1 eq, 2.0 mg, 0.0022 mmol) was added into a 10 mL Schleck tube with a stir bar. After three pump-purge cycles with high purity nitrogen to degas the tube, about 0.7 mL of CH₂Cl₂ was added to the tube to dissolve the catalyst. Then a solution of NbAzo in 1 mL of CH₂Cl₂ was injected quickly into the mixture. After the mixture was stirred at ambient temperature for 30 min, 0.1 mL of ethyl vinyl ether was added to terminate the polymerization. The reaction mixture was passed through a neutral alumina column to remove the catalyst and unreacted monomers. The filtrate was condensed and then precipitated into 100 mL of petroleum ether to afford a yellow solid.



Scheme S5. Synthesis of PAzo.

Doping of LiTFSI/NbAzo and Preparation of Azobenzene-Containing Electrolytes. PAzo, NbAzo, and LiTFSI were dissolved in 4 mL of THF, and the mixture was violently stirred for 24 h. The solution was passed through a filter membrane with a pore diameter of 0.22 μm . The filtrate was poured into a Teflon mold with a length of 3.0 cm and a width of 1.5 cm. After the solvent was evaporated at ambient temperature, the azobenzene-containing electrolyte membrane was formed.

Results

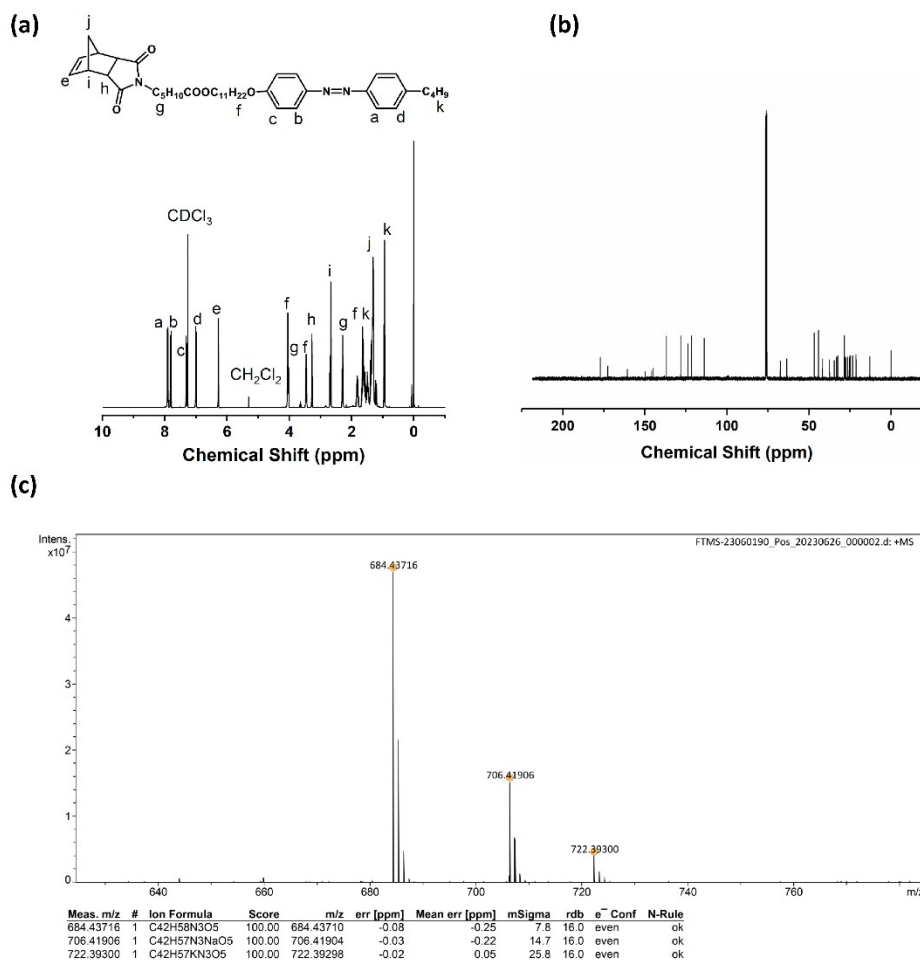


Figure S1. ^1H NMR (a), ^{13}C NMR (b), and MS (c) spectra of NbAzo.

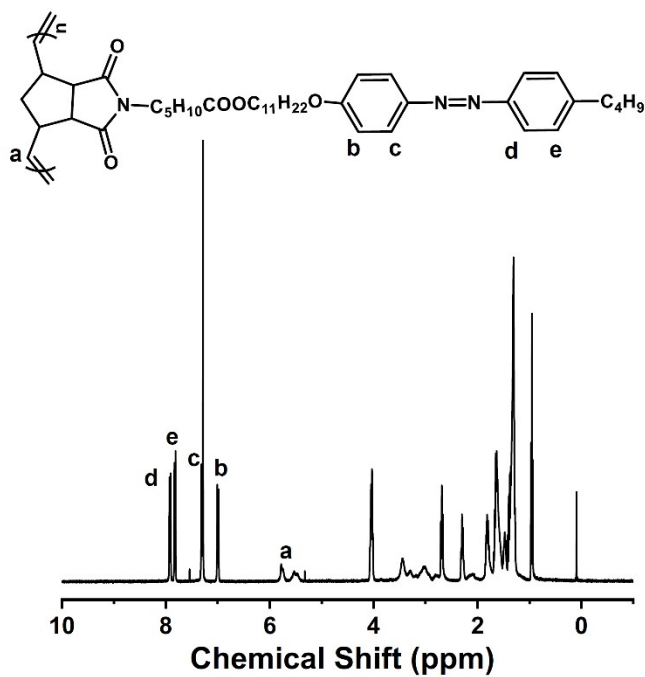


Figure S2. ¹H NMR spectrum of PAzo.

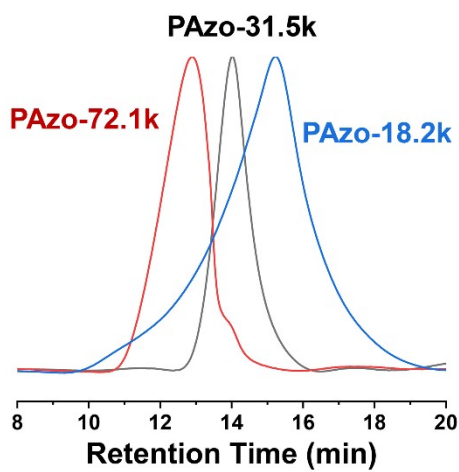


Figure S3. SEC traces of PAzo-18.2k, PAzo-31.5k, and PAzo-72.1k.

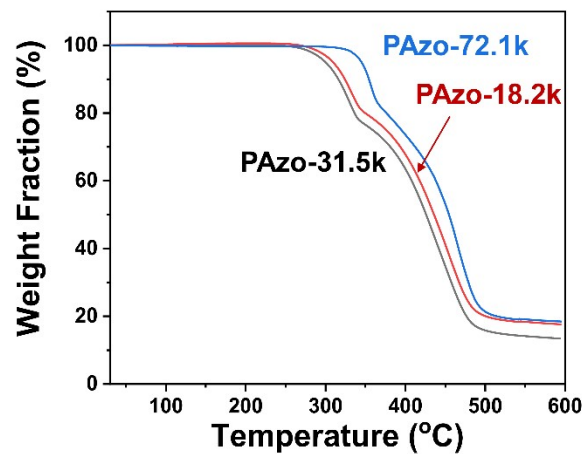


Figure S4. TGA thermograms of PAzo-18.2k, PAzo-31.5k, and PAzo-72.1k.

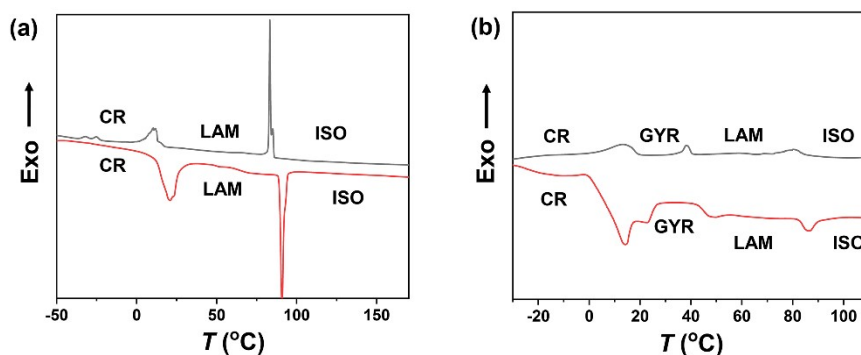


Figure S5. DSC curves of PAzo-31.5k (a) and PAzo-31.5k/NbAzo/LiTFSI ($r_{\text{Azo}} = 1.5$, $r_{\text{Li}} = 0.79$) (b) at a heating rate of $10 \text{ }^\circ\text{C min}^{-1}$ during the first cooling (black lines) and second heating (red lines).

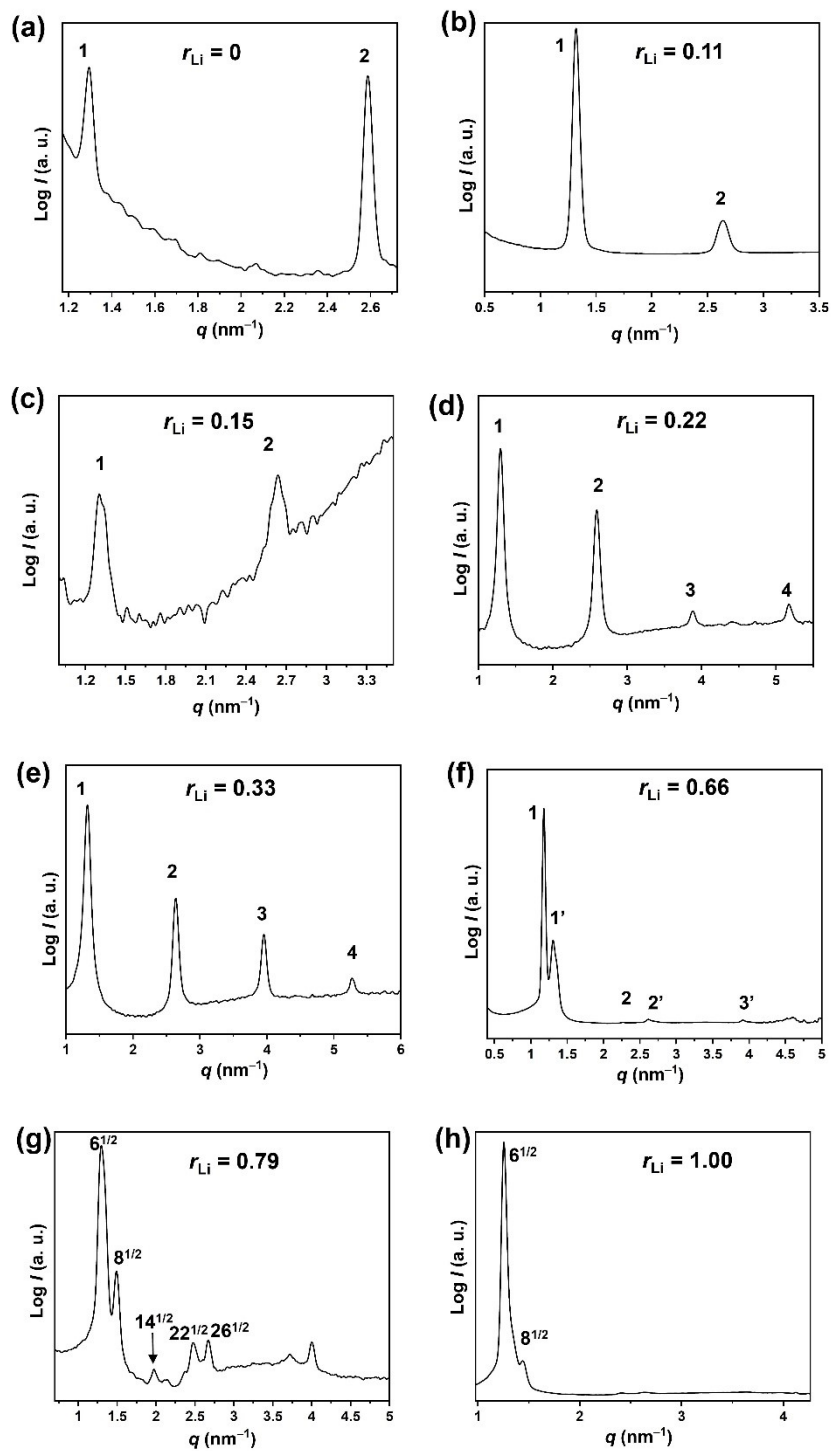


Figure S6. MAXS profiles of PAzo-31.5k/NbAzo/LiTFSI ($r_{\text{Azo}} = 1.5$) with r_{Li} of 0 (a), 0.11 (b), 0.15 (c), 0.22 (d), 0.33 (e), 0.66 (f), 0.79 (g), and 1.00 (h).

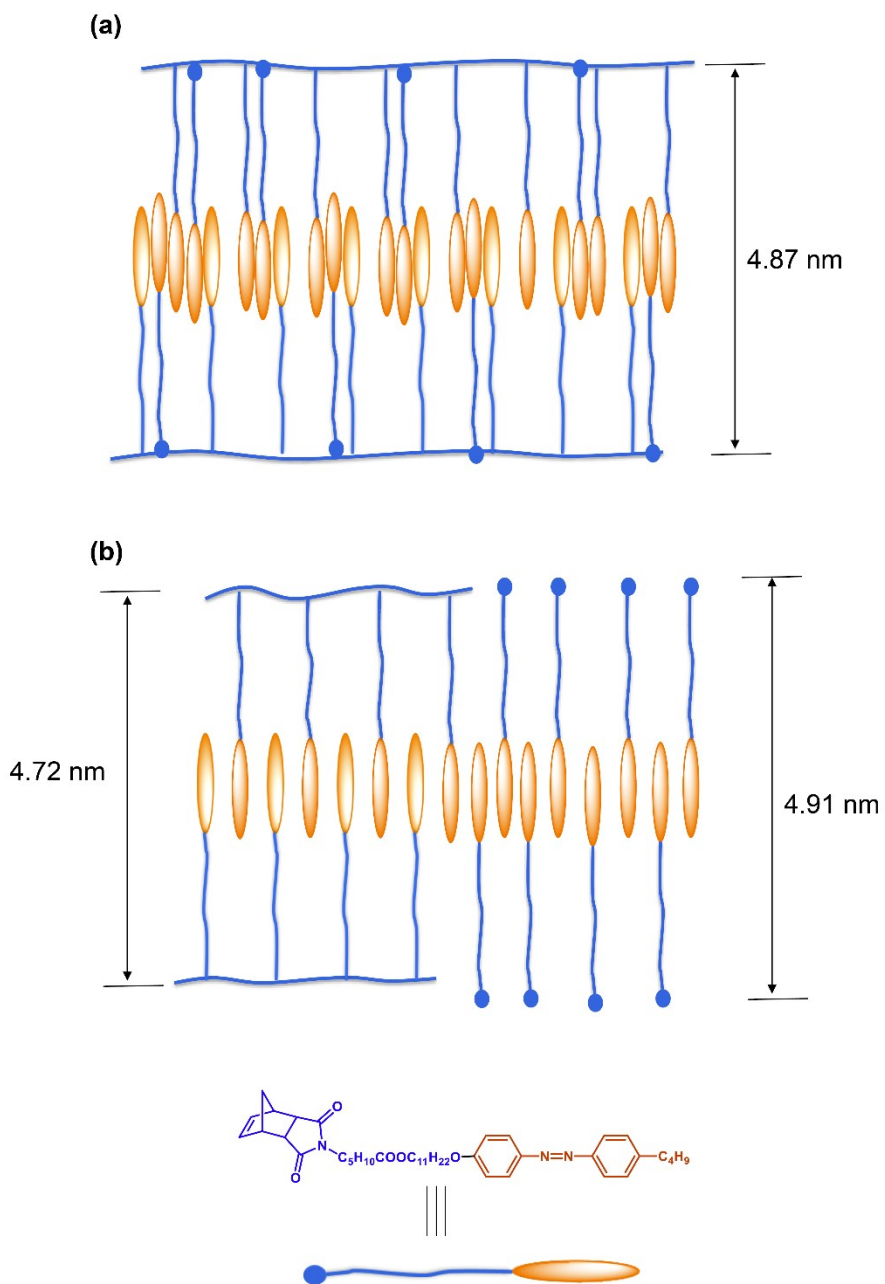


Figure S7. Schematic illustration of LAM (a) and LAM1 + LAM2 (b) structures formed by PAzo/NbAzo/LiTFSI.

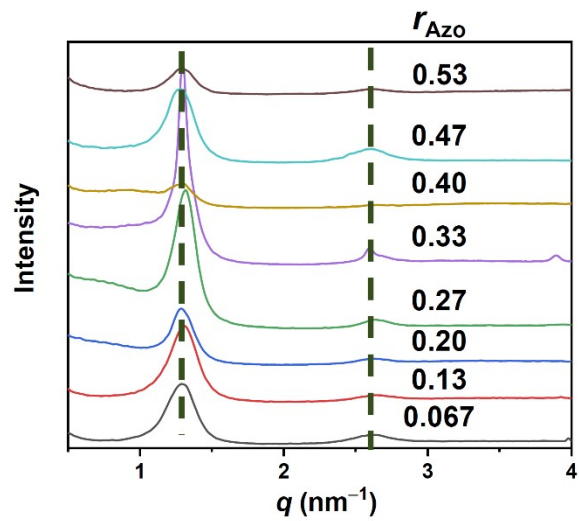


Figure S8 MAXS profiles of PAzo-315k/NbAzo/LiTFSI ($r_{Li} = 0.79$) with r_{Azo} of 0.067–0.53.

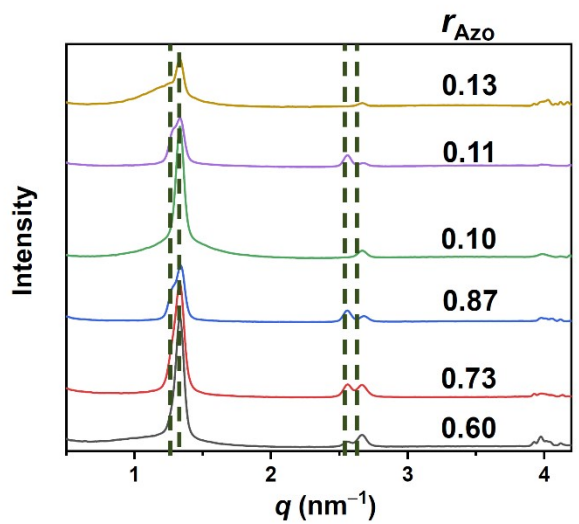


Figure S9. MAXS profiles of PAzo-315k/NbAzo/LiTFSI ($r_{Li} = 0.79$) with r_{Azo} of 0.60–1.30.

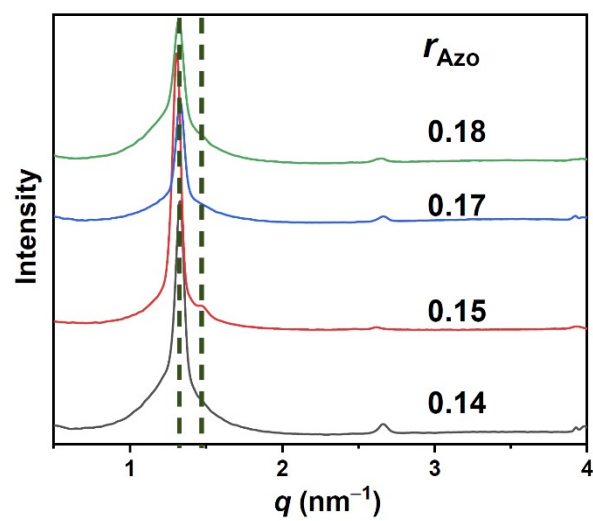


Figure S10. MAXS profiles of PAzo-315k/NbAzo/LiTFSI ($r_{Li} = 0.79$) with r_{Azo} of 1.40–1.80.

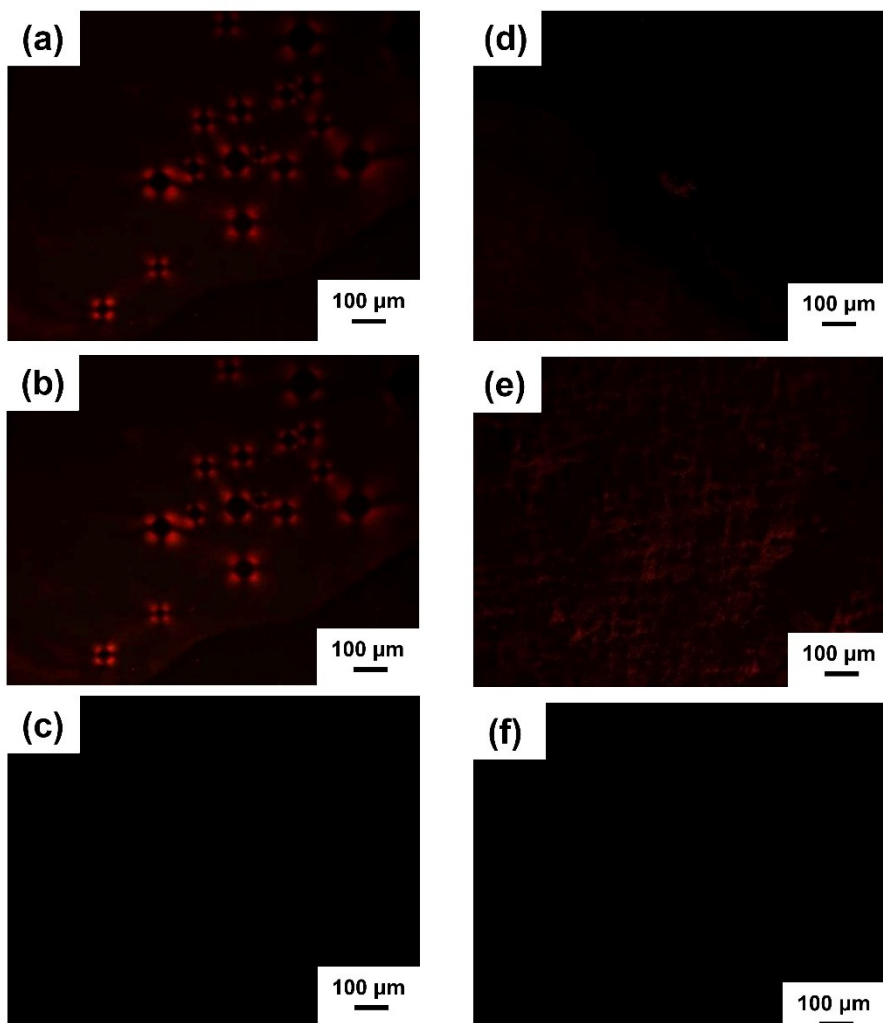


Figure S11. PLM results of PAzo-31.5k at 20 (a), 50 (b), and 100 (c) °C and PAzo-31.5k/NbAzo/LiTFSI ($r_{\text{Azo}} = 1.5$, $r_{\text{Li}} = 0.79$) at 30 (d), 60 (e), and 100 (f) °C.

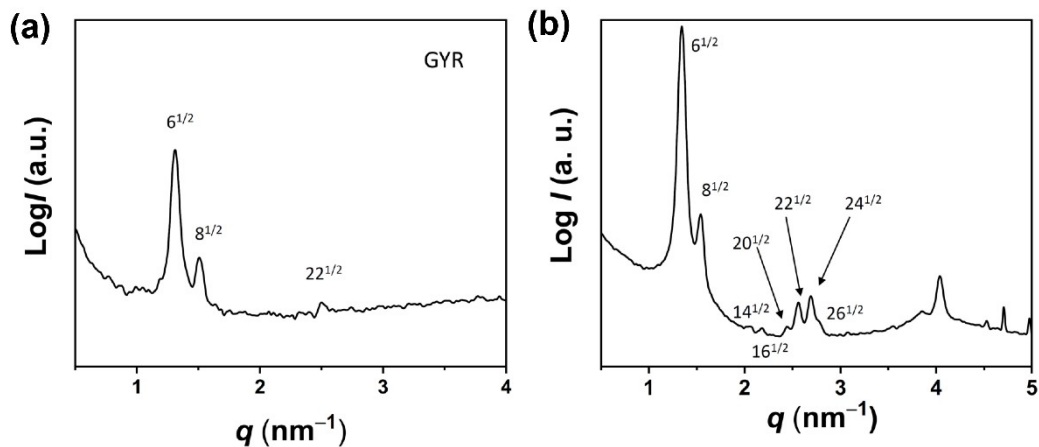


Figure S12. MAXS profiles of PAzo-72.1k/NbAzo/LiTFSI ($r_{\text{Azo}} = 1.5$, $r_{\text{Li}} = 0.79$) (a) and PAzo-63.2k/NbAzo/LiTFSI ($r_{\text{Azo}} = 1.5$, $r_{\text{Li}} = 0.79$) (b).

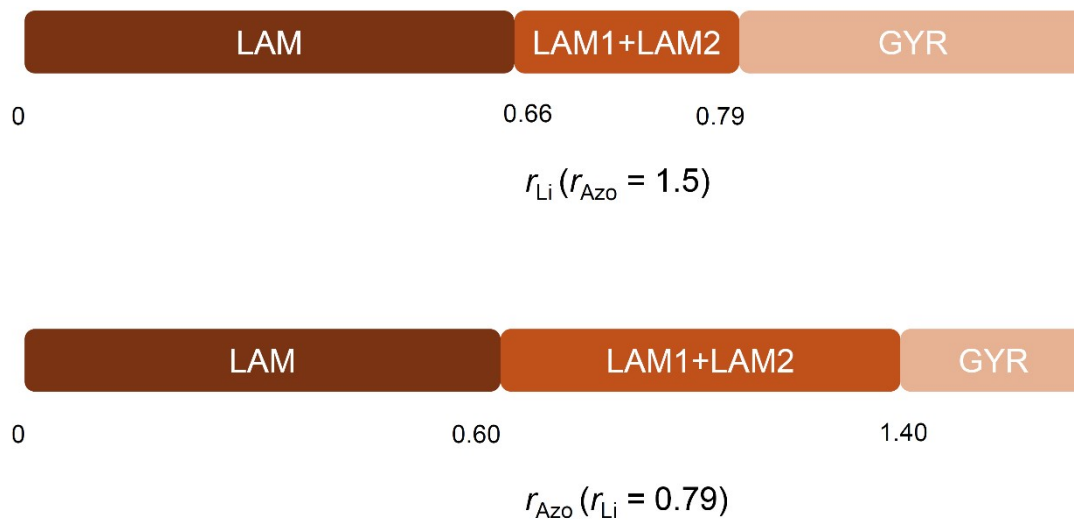


Figure S13. Apparent phase diagrams of PAzo/NbAzo/LiTFSI with different r_{Li} (a) and r_{Azo} (b) values.

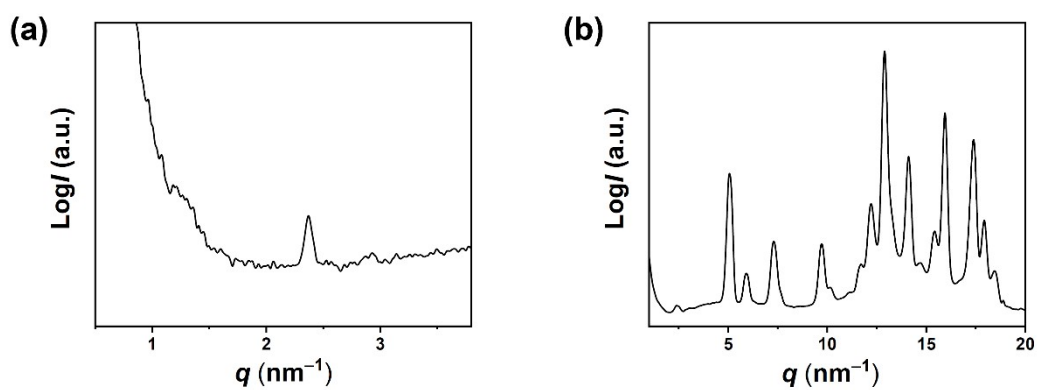


Figure S14. MAXS (a) and WAXS (b) profiles of NbAzo.

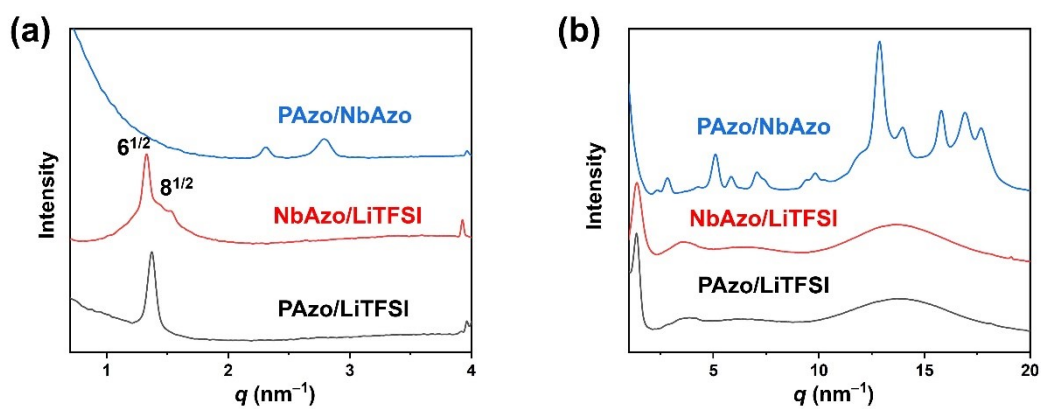


Figure S15. MAXS (a) and WAXS (b) profiles of PAzo-18.2k/LiTFSI ($r_{Li} = 0.79$), NbAzo/LiTFSI, and PAzo-18.2k/NbAzo ($r_{Azo} = 1.5$).

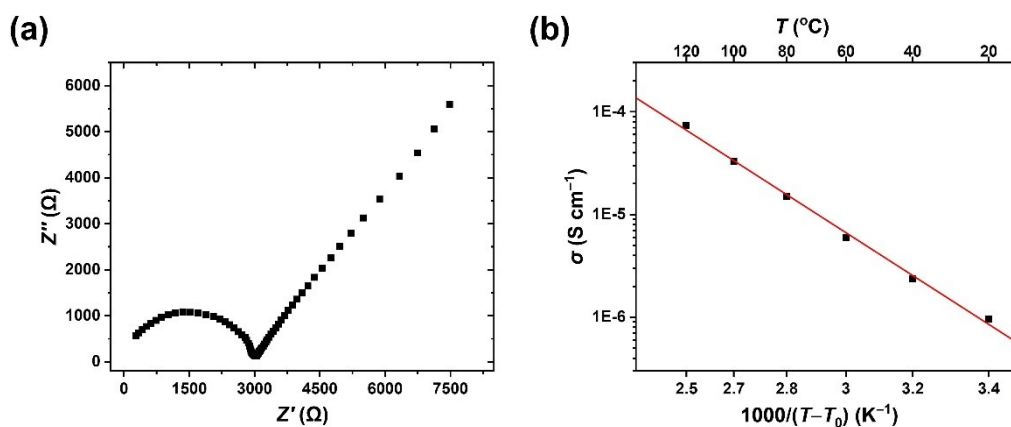


Figure S16. The Nyquist curve of PAzo-18.2k/NbAzo/LiTFSI ($r_{\text{Azo}} = 1.5$, $r_{\text{Li}} = 0.66$) at ambient temperature (a) and temperature-dependent ionic conductivities of PAzo-18.2k/NbAzo/LiTFSI ($r_{\text{Azo}} = 1.5$, $r_{\text{Li}} = 0.66$) fitted with the Arrhenius equation (b).

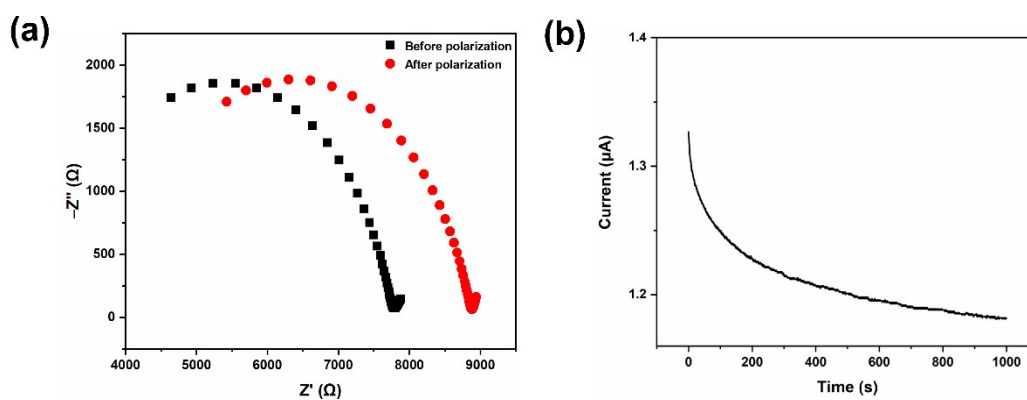


Figure S17. The Nyquist curve of PAzo-31.5k/NbAzo/LiTFSI ($r_{\text{Azo}} = 1.5$, $r_{\text{Li}} = 0.79$) before and after polarization (a) and time-current diagram (b: polarization voltage at 10 mV, 25 °C).